

Aldo-keto reductase and alcohol dehydrogenase contribute to benznidazole natural resistance in *Trypanosoma cruzi*

Laura González,^{1†} Paola García-Huertas,^{1†}
Omar Triana-Chávez ,¹ Gabriela Andrea García,²
Silvane Maria Fonseca Murta³ and
Ana M. Mejía-Jaramillo ^{1*}

¹Grupo Biología y Control de Enfermedades Infecciosas-BCEI, Universidad de Antioquia, UdeA, Medellín, Colombia.

²Instituto Nacional de Parasitología “Dr. Mario Fatala Chaben”- ANLIS “Dr. Carlos G. Malbrán”, Buenos Aires, Argentina.

³Centro de Pesquisas René Rachou, Fiocruz/MINAS, Brasil.

Summary

The improvement of Chagas disease treatment is focused not only on the development of new drugs but also in understanding mechanisms of action and resistance to drugs conventionally used. Thus, some strategies aim to detect specific changes in proteins between sensitive and resistant parasites and to evaluate the role played in these processes by functional genomics. In this work, we used a natural *Trypanosoma cruzi* population resistant to benznidazole, which has clones with different susceptibilities to this drug without alterations in the *NTR I* gene. Using 2DE-gel electrophoresis, the aldo-keto reductase and the alcohol dehydrogenase proteins were found up regulated in the natural resistant clone and therefore their possible role in the resistance to benznidazole and glyoxal was investigated. Both genes were over-expressed in a drug sensitive *T. cruzi* clone and the biological changes in response to these compounds were evaluated. The results showed that the overexpression of these proteins enhances resistance to benznidazole and glyoxal in *T. cruzi*. Moreover, a decrease in mitochondrial and cell membrane damage was observed, accompanied by a drop in the intracellular concentration of reactive oxygen species after treatment. Our results suggest that these

proteins are involved in the mechanism of action of benznidazole.

Introduction

Chagas disease, caused by the parasite *T. cruzi*, remains a public health problem in Latin America, with approximately five million people infected and 13% at risk of infection (WHO, 2015a). Additionally, the disease has been reported in non-endemic countries, such as the United States, Canada, Australia, Japan and some European countries due to migration and tourism, which increases the risk of infection by nonvectorial transmission routes such as blood transfusion, organ transplantation, and congenital infection in these countries (Schmunis, 2007; WHO, 2015b).

Treatment is limited to two nitroheterocyclic agents: benznidazole (Bz) and nifurtimox (Nfx). Unfortunately, the chemotherapy results are unsatisfactory because of multiple side effects (Coura Rodriguez and de Castro, 2002; Apt and Zulantay, 2011), and the low percentage cure rate mainly during the chronic phase of the disease (Marin-Neto *et al.*, 2009; WHO, 2015b). Additionally, some studies have shown low efficacy of treatment due to the presence of naturally drug-resistant parasites in patients (Filardi and Brener, 1987; Cançado, 1999; Coronado *et al.*, 2006).

The occurrence of Bz and Nfx resistant parasites has been detected in at least 27% of the strains isolated from different geographic and biological origins (Filardi and Brener, 1987). This type of resistance is known as natural resistance, and is based on the fact that the organism has a particular trait that allows some members of the population to survive changes in the environment and eventually to the drugs. In this resistance type, the special attribute is present in the organism before is treated (Hayes and Wolf, 1990). Additionally, it has been found that sensitive strains or clones exposed to constant pressures of Bz or Nfx gain resistance (Wilkinson *et al.*, 2008; Mejía *et al.*, 2012). Induced drug resistance arises in a population (Murta *et al.*, 1998, 2008; Mejía *et al.*, 2012) or clone (Wilkinson *et al.*, 2008) that was initially susceptible to the drug, because

Accepted 4 September, 2017. *For correspondence. E-mail maria.mejia3@udea.edu.co; Tel. (+574) 2196520; Fax (+574) 2196521. †These authors contributed equally to this article.

gradual and long term exposure to the drug induces damages (point mutations or allelic losses) in one or more genes related to the mechanism of action of the drug, leading to the resistance phenotype (Wilkinson *et al.*, 2008; Mejía *et al.*, 2012; Campos *et al.*, 2014).

Currently, some studies focused on understanding the mechanisms by which the parasites become resistant have identified genes such as mitochondrial NADH - dependent type-I nitroreductase (*NTR I*) (Wilkinson *et al.*, 2008; Mejía *et al.*, 2012; Campos *et al.*, 2014), which play critical role in the activation pathways of both drugs, leading to the formation of glyoxal (GO), a highly reactive metabolite, which generates guanosine-glyoxal adducts (Hall and Wilkinson, 2012). Functional studies have demonstrated that the expression of this enzyme is key to the trypanocidal properties displayed by the Bz, since the inactivation by allelic loss and point mutations confers resistance to this drug (Wilkinson *et al.*, 2008; Mejía-Jaramillo *et al.*, 2011; Hall and Wilkinson, 2012; Mejía *et al.*, 2012; Kelly and Wilkinson, 2013). Intriguingly, alterations in the *NTR I* gene were not found in Bz resistant parasites isolated from humans (Mejía *et al.*, 2012), suggesting the participation of other genes in this process.

In this context, in the present work, we obtained clones from one of these resistant strains and analyzed the differential expression of genes by 2DE-gel electrophoresis in two clones with different susceptibility to Bz. Interestingly, we found that two *T. cruzi* proteins previously described to be related to Bz resistance, the aldo-keto reductase (TcAKR) and alcohol dehydrogenase (TcADH), were overexpressed in the resistant clone. Recently, Garavaglia *et al.* (2016) found that the overexpression of TcAKR in epimastigotes increased the resistance to Bz but it is irrelevant in the Bz detoxification in natural resistance strains (Garavaglia *et al.*, 2016). Likewise, Campos *et al.* (2009) showed that TcADH has a decreased level of expression *in vitro* induced Bz-resistant *T. cruzi* population, but not *in vivo* selected Bz-resistant and naturally resistant strains (Campos *et al.*, 2009). Therefore, the poor knowledge regarding the role of TcAKR and TcADH in Bz natural resistance lead us to further characterize the function of these enzymes in *T. cruzi*.

Results

DA strain has clones with different susceptibilities to Bz

Five clones (cl1-cl5) obtained from the DA strain with EC_{50} to Bz of $10.95 \pm 2.2 \mu\text{M}$, $26.90 \pm 3.0 \mu\text{M}$, $29.20 \pm 2.1 \mu\text{M}$, $34.40 \pm 2.9 \mu\text{M}$ and $49.54 \pm 3.3 \mu\text{M}$ were analyzed. The genetic characterization by LSSP-

PCR and RAPDs showed 8 polymorphic bands between all the clones with 100% of the band shared between clones cl1 ($EC_{50} = 10.95 \mu\text{M}$) and cl5 ($EC_{50} = 49.54$) (Supporting Information Fig. S1). These two clones were considered as sensitive (DA-S, cl1) and resistant (DA-R, cl5) to Bz, based on their EC_{50} , as compared with previous reports (Mejía *et al.*, 2012). In the absence of drug treatment, both clones grew at a comparable rate in culture (Fig. 1A). However, infection assays showed that the DA-R clone had a 2.7 times lower infection rate than DA-S ($P < 0.001$; Fig. 1B), although the number of amastigotes per cell was not affected.

*The EC_{50} ratio of Bz between sensitive and resistant clones is maintained throughout the life cycle of *T. cruzi**

In order to assess if the ratio of Bz between DA-S and DA-R clones was maintained throughout their life cycle, the susceptibility to the drug in intracellular amastigotes and trypomastigotes was determined for both clones. The results showed that the EC_{50} to Bz of the amastigotes and trypomastigotes was lower in the sensitive clone than the resistant one, and the EC_{50} ratio to Bz between both clones was similar, approximately 4.0, in all the parasitic stages (Table 1).

*The *NTR I* gene is not affected in the DA-R clone*

With prior knowledge that the point mutations and loss of one allele in the *NTR I* gene changes the sensitivity to Bz, the sequences and the mRNA levels of this gene were analyzed in both clones and compared with previous reports (Mejía-Jaramillo *et al.*, 2011; Mejía *et al.*, 2012). In the first parameter, we did not find changes in the *NTR I* gene sequence between DA-S (GenBank accession no. MF289089) and DA-R (GenBank accession no. MF289090), and neither with the DA strain (GenBank accession no. JN043344) and the sensitive clone 61S (GenBank accession no. MF289091). Additionally, we could not find the previously reported point mutations of the resistant clones 61R-3, 61R-4, 61R-6 in these clones (GenBank accession no. MF289092, MF289093 and MF289094 respectively) (Supporting Information Fig. S2A). Moreover, the mRNA levels were not significant different between both clones (Supporting Information Fig. S2B).

TcAKR and TcADH proteins were overexpressed in the resistant clone

Given that we did not find evident changes in the *NTR I* gene between DA-S and DA-R clones that could explain

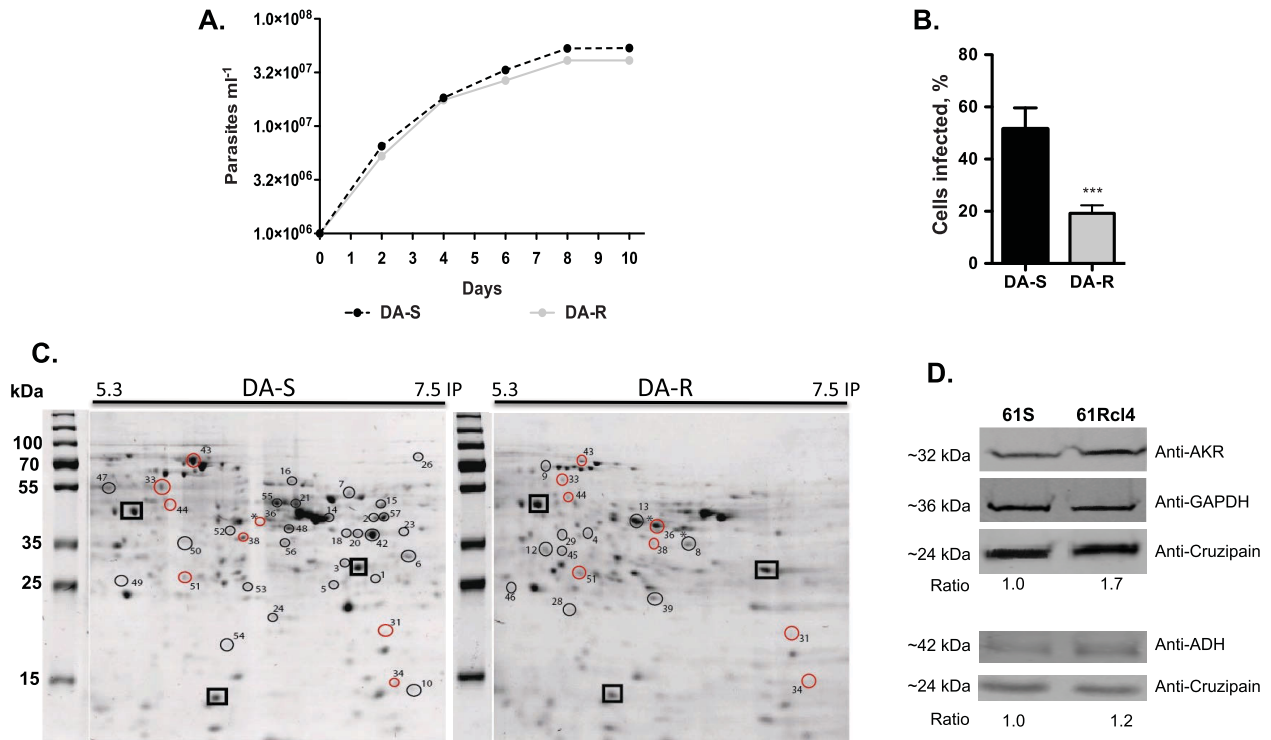


Fig. 1. Biological and molecular characterization of *T. cruzi* sensitive (black) and resistant (gray) clones.

A. Cumulative cell density of DA-S and DA-R clones; Epimastigotes from sensitive and resistant clones were counted every two days for 10 days by triplicate.

B. Infection of VERO cells with DA-S and DA-R clones stained with Giemsa. Cell-derived trypomastigotes were added to a VERO cell monolayer at a 6:1 ratio of parasite/host cell. Infected cells were counted after 72 h. Experiments were performed in triplicate, with data presented as the means \pm SD; a total of 500 cells were counted. * $P < 0.05$ ** $P < 0.01$ *** $P < 0.001$.

C. Proteomic analysis in 2D-gels of the DA-S and DA-R clone. The IPG strips were placed into a 12% polyacrylamide gel and run in a Mini-PROTEAN Tetra Cell and then stained with Coomassie blue G-250. The squares represent the landmarks used to align all gels. Black circles are the exclusively expressed proteins in either one of the clones, and red circles represent the differential expressed proteins between both clones. The asterisks show the spots corresponding to TcAKR (8) and TcADH (36) proteins.

D. Analysis of TcAKR and TcADH proteins expression by Western blotting in epimastigotes of *T. cruzi* sensitive (61S) and induced resistant (61Rcl4) clones using mouse anti-rTcAKR polyclonal serum (1:500) and rabbit anti-rTcADH polyclonal serum (1:500) respectively, with rabbit anti-cruzipain polyclonal serum (1:500) and mouse anti-GAPDH polyclonal serum (1:300) as a loading control. The numbers in the bottom of the membranes correspond to the fold of expression compared with the loading controls and analyzed by densitometry using the ImageJ software.

the difference in Bz resistance, we decided to analyze their proteomes with the aim of identifying new proteins involved in this phenotype (Fig. 1C).

After comparing a total of 363 spots obtained from the 2D-gels, it was revealed that 45 spots had significant differences ($P \leq 0.05$), 37 were exclusively expressed proteins (27 were present only in the sensitive clone and 10 in the resistant one), 4 were downregulated in the resistant clone, and 4 were overexpressed in this same clone (Table 2).

Functional annotation showed that the differentially expressed genes were mainly associated with protein binding, heterocyclic compound binding and oxidoreductase activity, among other functions. Interestingly, just a few proteins were found to be exclusively expressed or up regulated in the resistant clone. Inside this group, we discard proteins as enolase or heat shock proteins due they are frequently found in 2D-gels without significant role in the study's hypotheses (Petraik *et al.*, 2008). Other proteins as

Table 1. *In vitro* susceptibility to Bz of three different stages of DA-S and DA-R *T. cruzi* clones.

| | Epimastigotes | | Amastigotes | | Trypomastigotes | |
|------|--------------------------|----------------|--------------------------|----------------|--------------------------|----------------|
| | Mean \pm SD (μ M) | Ratio R/S | Mean \pm SD (μ M) | Ratio R/S | Mean \pm SD (μ M) | Ratio R/S |
| DA-S | 10.95 \pm 2.2 | 4.52 \pm 1.5 | 1.44 \pm 1.1 | 4.14 \pm 1.3 | 3.63 \pm 1.6 | 3.61 \pm 0.6 |
| DA-R | 49.54 \pm 3.3 | | 5.96 \pm 1.4 | | 13.09 \pm 0.9 | |

Table 2. Protein identification by Matrix Science Mascot program.

| Number of spot | Best protein description | TrypIDB ID | pl obser (theo) | MW obser (theo) | P value | Expression in resistant clone |
|----------------|--|-------------------------|-----------------|-----------------|------------|-------------------------------|
| 1 | Adenine phosphoribosyltransferase [<i>Trypanosoma cruzi</i> strain CL Brener] | Tc00.1047053507519.140 | 7.06 (7.32) | 26 (25.86) | 0.00000305 | Absent |
| 2 | Protein disulfide isomerase, putative [<i>Trypanosoma cruzi</i>] | Tc00.1047053508209.140 | 7.16 (7.18) | 41 (41.87) | 0.000043 | |
| 3 | 6-phosphogluconolactonase, putative [<i>Trypanosoma cruzi</i>] | Tc00.1047053503945.40 | 6.97 (6.84) | 30 (28.70) | 0.0000484 | |
| 5 | Phosphomannomutase [<i>Trypanosoma cruzi</i> strain CL Brener] | Tc00.1047053510187.480 | 6.87 (6.41) | 25 (28.21) | 0.0000851 | |
| 10 | Ribose 5-phosphate isomerase, putative [<i>Trypanosoma cruzi</i>] | Tc00.1047053508601.119 | 7.44 (7.11) | 14 (17.28) | 0.000548 | |
| 50 | Alpha tubulin [Parabodo caudatus] | - | 5.9 (nd) | 36 (38.12) | 0.001 | |
| 14 | Dehydrogenase [<i>Trypanosoma cruzi</i>] | Tc00.1047053508461.80 | 6.79 (6.43) | 42 (42.19) | 0.00156 | |
| 20 | RNA-binding protein RGm, putative [<i>Trypanosoma cruzi</i>] | Tc00.1047053503419.50 | 7.06 (9.31) | 37 (34.65) | 0.0016 | |
| 15 | Cystathionine beta-synthase [<i>Trypanosoma cruzi</i> strain CL Brener] | Tc00.1047053511691.10 | 7.01 (7.32) | 48 (43.19) | 0.00177 | |
| 16 | 3-hydroxy-3-methylglutaryl-CoA synthase, putative | Tc00.1047053511903.40 | 6.61 (6.59) | 59 (54.72) | 0.0028 | |
| 18 | Cytosolic malate dehydrogenase [<i>Trypanosoma cruzi</i> strain CL Brener] | Tc00.1047053506937.10 | 6.99 (6.66) | 37 (35.57) | 0.0036 | |
| 54 | Co-chaperone GrpE [<i>Trypanosoma cruzi</i> strain CL Brener] | Tc00.1047053509045.20 | 6.1 (8.90) | 18 (24.35) | 0.0053 | |
| 57 | L-threonine 3-dehydrogenase [<i>Trypanosoma cruzi</i> strain CL Brener] | Tc00.1047053507923.10 | 7.23 (7.20) | 43 (36.88) | 0.0053 | |
| 21 | Enolase [<i>Trypanosoma cruzi</i> strain CL Brener] | Tc00.1047053504105.140 | 6.65 (6.20) | 49 (46.42) | 0.0056 | |
| 49 | I/6 autoantigen, putative [<i>Trypanosoma cruzi</i>] | Tc00.1047053508323.100 | 5.4 (4.92) | 26 (23.00) | 0.0057 | |
| 52 | hypothetical protein HMPREF1006.01961 [Synergistes sp. 3_1_syn1] | - | 6.2 (nd) | 39 (10.83) | 0.0065 | |
| 53 | selA gene product [Helicobacter pylori F32] | - | 6.32 (nd) | 23 (43.82) | 0.0067 | |
| 23 | IgG-immunoreactive zinc finger protein [Strongyloides stercoralis] | - | 7.35 (6.7) | 38 (36.62) | 0.0073 | |
| 24 | Co-chaperone GrpE [<i>Trypanosoma cruzi</i> strain CL Brener] | Tc00.1047053509045.20 | 6.09 (8.95) | 21 (24.35) | 0.008 | |
| 55 | Tyrosine aminotransferase | Tc00.1047053510187.50 | 6.14 (6.14) | 49 (46.12) | 0.0089 | |
| 7 | Dihydrolipeoyl dehydrogenase, putative | Tc00.1047053511025.110 | 6.9 (7.46) | 52 (50.58) | 0.0148 | |
| 47 | Heat shock protein 60 | Tc00.1047053507641.290 | 5.4 (5.14) | 54 (59.13) | 0.0168 | |
| 48 | Proline racemase:B-cell mitogen precursor, putative | Tc00.1047053430737.10 | 6.60 (6.62) | 39 (44.07) | 0.0168 | |
| 26 | Urocanate hydratase [<i>Trypanosoma cruzi</i> strain CL Brener] | TcCLB504045.110 | 7.44(6.75) | 77 (74.72) | 0.0187 | |
| 6 | Alpha S1 casein, partial [Bos taurus] | Tc00.1047053511411.8 | 7.4 (9.02) | 31 (23.47) | 0.02 | |
| 42 | Electron-transfer-flavoprotein, alpha polypeptide, putative [<i>Trypanosoma cruzi</i>] | Tc00.1047053503559.109 | 7.2 (8.93) | 38 (33.46) | 0.05 | |
| 56 | Enolase [<i>Trypanosoma cruzi</i> strain CL Brener] | Tc00.1047053504105.140 | 6.6 (6.20) | 36 (46.42) | 0.05 | |
| 13 | Enolase [<i>Trypanosoma cruzi</i> strain CL Brener] | Tc00.1047053504105.140 | 6.0 (6.20) | 46 (46.42) | 0.0000143 | Exclusive |
| 4 | Heat shock 70 kDa protein, mitochondrial precursor [<i>Trypanosoma cruzi</i>] | Tc00.1047053507029.30 | 5.88 (5.71) | 36 (70.95) | 0.0000799 | |
| 8 | Aldo-keto reductase | Tc00.1047053511287.49 | 6.5 (7.96) | 35 (32.5) | 0.0003933 | |
| 9 | Transitional endoplasmic reticulum ATPase, putative [<i>Trypanosoma cruzi</i>] | Tc00.1047053509733.170 | 5.52 (5.23) | 71 (86.06) | 0.000491 | |
| 45 | Gart [Drosophila yakuba] | - | 5.6 (nd) | 31 (12.97) | 0.0117 | |
| 39 | Glycosyltransferase [SAR116 cluster alpha proteobacterium HIMB100] | Tc00.1047053511211.170 | 6.3 (nd) | 23 (42.66) | 0.0196 | |
| 28 | Heat shock protein HSP70 [<i>Trypanosoma cruzi</i>] | Tc00.1047053506937.10 | 5.56 (5.22) | 20 (71.19) | 0.026 | |
| 29 | Cytosolic malate dehydrogenase, putative [<i>Trypanosoma cruzi</i>] | Tc00.1047053411235.9 | 5.66 (6.66) | 35 (35.59) | 0.0277 | |
| 12 | Tubulin, alpha 4 like [Danio rerio] | Tc00.1047053411235.9 | 5.5 (4.70) | 31 (49.79) | 0.0317 | |
| 46 | Tryparedoxin peroxidase [<i>Trypanosoma cruzi</i> strain CL Brener] | Tc00.1047053509499.14 | 5.3 (5.10) | 24 (25.49) | 0.0369 | |
| 43 | heat shock 70 kDa protein [<i>Trypanosoma cruzi</i> strain CL Brener] | Tc00.1047053511211.170 | 5.8 (5.22) | 70 (73.29) | 0.036 | Down |
| 33 | hypothetical protein TCSYL10_2103 [<i>Trypanosoma cruzi</i>] | Tc00.1047053510947.30 | 5.74 (5.07) | 56 (48.62) | 0.037 | |
| 44 | peptidase T [<i>Trypanosoma cruzi</i> strain CL Brener] | Tc00.10470535066513.110 | 5.7 (4.98) | 50 (46.44) | 0.044 | |
| 38 | Activated protein kinase C receptor [<i>Trypanosoma cruzi</i> strain CL Brener] | Tc00.1047053511211.120 | 6.24 (6.04) | 36 (35.01) | 0.05 | |
| 51 | Nitrilase [<i>Trypanosoma cruzi</i> strain CL Brener] | Tc00.1047053510039.40 | 5.8 (5.66) | 27 (30.84) | 0.0089 | Up |
| 31 | Peak not detected | - | 7.19 (-) | 19 (-) | 0.035 | |
| 34 | Predicted: keratin, type I cytoskeletal 10 [Pan paniscus] | - | 7.1 (-) | 14 (54) | 0.038 | |
| 36 | Alcohol dehydrogenase, putative [<i>Trypanosoma cruzi</i>] | Tc00.1047053506357.50 | 6.32 (6.5) | 40 (41.79) | 0.048 | |

tryparedoxin peroxidase have been broadly studied in trypanosomatids and their role in resistance was unambiguously showed in other studies (Nogueira *et al.*, 2009; Wyllie *et al.*, 2010). Hence, we selected two proteins, TcAKR (spot 8, Fig. 1C) and TcADH (spot 36, Fig. 1C), to confirm their role in Bz resistance using transgenic parasites. TcAKR was found as exclusively expressed in the resistant clone with an isoelectric point (IP) of 6.5 and a molecular weight of 35 kDa; and TcADH was fourfold more abundant in the resistant clone, with an IP of 6.32 and a molecular weight of 40 kDa. Moreover, these enzymes were selected based on their inconclusive role found in the *T. cruzi* Bz resistance (Campos *et al.*, 2009; Garavaglia *et al.*, 2016) and the confirmed role in GO resistance found in other organism such as bacteria, yeast and humans (Shangari and O'Brien, 2004; Barski *et al.*, 2008; Hoon *et al.*, 2011; Penning, 2014a, 2014b).

In addition, to support the choice of these enzymes and their possible function in the resistance to Bz, we evaluated the expression of these two proteins by western blot in Bz induced resistance *T. cruzi* 61R-4 clone compared to the 61S sensitive clone. Our finding showed a slightly increase in the ADH and AKR proteins expression (1.2 and 1.7-fold respectively) in the induced resistance clone (Fig. 1D).

Mutations in TcAKR and TcADH genes are not exclusive in the resistant clones

Since in *T. cruzi* is frequent to find mutations in genes involved in the resistance to Bz (Mejía *et al.*, 2012), we analyzed the sequence of the *TcAKR* and *TcADH* genes in these 2 clones and those previous mentioned 61S, 61R-3 and 61R-4, and compared them with available sequences in the TriTrypDB (tritrypdb.org) from CLBrenner, Sylvio and DM28c strains. For TcAKR, we did not find changes in the amino acid sequences among sensitive and resistant clones except for positions 51 and 52 that were observed in 61R-3 and 61R-4 clones; but these polymorphisms were shared with CLBrenner. In the same way, TcADH sequences were similar for all the clones used except for position 214 for 61R-4. Thus, changes in the nucleotide or amino acid sequences between DA-S and DA-R clones were not found. Therefore, the observed differences in the expression of these proteins between both clones are not due to mutations (Supporting Information Fig. S3).

Overexpression of TcAKR and TcADH increases the resistance to Bz and GO in T. cruzi

After transfection of both genes in *T. cruzi* 61S clone, we found that the levels of *TcAKR* and *TcADH* mRNA

in the transfected parasites were approximately threefold higher than the control parasites transfected with pTEX-GFP ($P < 0.001$; Fig. 2A). In concordance with this result, the level of protein increased around twofold and fourfold in the transfected parasites with *TcAKR* and *TcADH* genes respectively (Fig. 2B). At this level of overexpression, no change was observed in the *in vitro* growth of both transfected parasites (Fig. 2C) and neither obvious morphological change was evidenced.

To demonstrate whether overexpression of TcAKR and TcADH alter the effect of Bz and GO in *T. cruzi*, we compared the response of these parasites after being treated with these compounds. Interestingly, our results showed that parasites overexpressing TcAKR or TcADH are more resistant to Bz and GO. The Bz EC₅₀ values calculated by MTT methodology for both transfected parasites pTEX-TcAKR and pTEX-TcADH were approximately twofold higher (12.3 ± 0.6 and 13.93 ± 1.5 μ M respectively) and significantly different ($P < 0.001$) than the control parasites (EC₅₀ of 7.11 ± 1.1 μ M). However, as we could not calculate the EC₅₀ of GO by this methodology due to reduction of MTT by this product, we counted the parasites in the cytometry chamber using the erythrosine-b after 24 h of treated them with different concentrations of this compound. The EC₅₀ obtained by this methodology were of 8.05 ± 0.6 , 10 ± 0.08 and 12.4 ± 0.05 mM GO for pTEX-GFP, pTEX-TcAKR and pTEX-TcADH respectively, and significant different between the first one and the others ($P < 0.0001$). Interestingly, at 30 mM GO we found the largest differences in the survival rate (twofold) between them. To better understand the possible function in the resistance of these two proteins, we followed the growth of parasites in the presence of both compounds for several days (Fig. 3). Thus, in the presence of 60 μ M Bz, parasites overexpressing TcAKR and TcADH grew 1.8-fold and 1.5-fold more respectively than the control ($P < 0.05$), with significantly different growth from day 1 to 5 and day 1 to 10 respectively ($P < 0.05$; Fig. 3A and B). On the same way, pTEX-TcAKR and pTEX-TcADH parasites treated with 30 mM GO showed viable parasites after day 5 when the parasites from the control were already dead. Additionally, it was a significantly increase in growth of these parasites of 6.1- and 2.1-fold more than the control respectively ($P < 0.05$; Fig. 3C and D).

Cell viability evaluated by DiOC6 and PI staining showed that cell death in the Bz-treated pTEX-GFP parasites occurs primarily at 96 h, decreasing by 40% after seven days. When we analyzed the pTEX-TcAKR and pTEX-TcADH parasites, we found a significant increase ($P < 0.05$) in cell viability compared to the

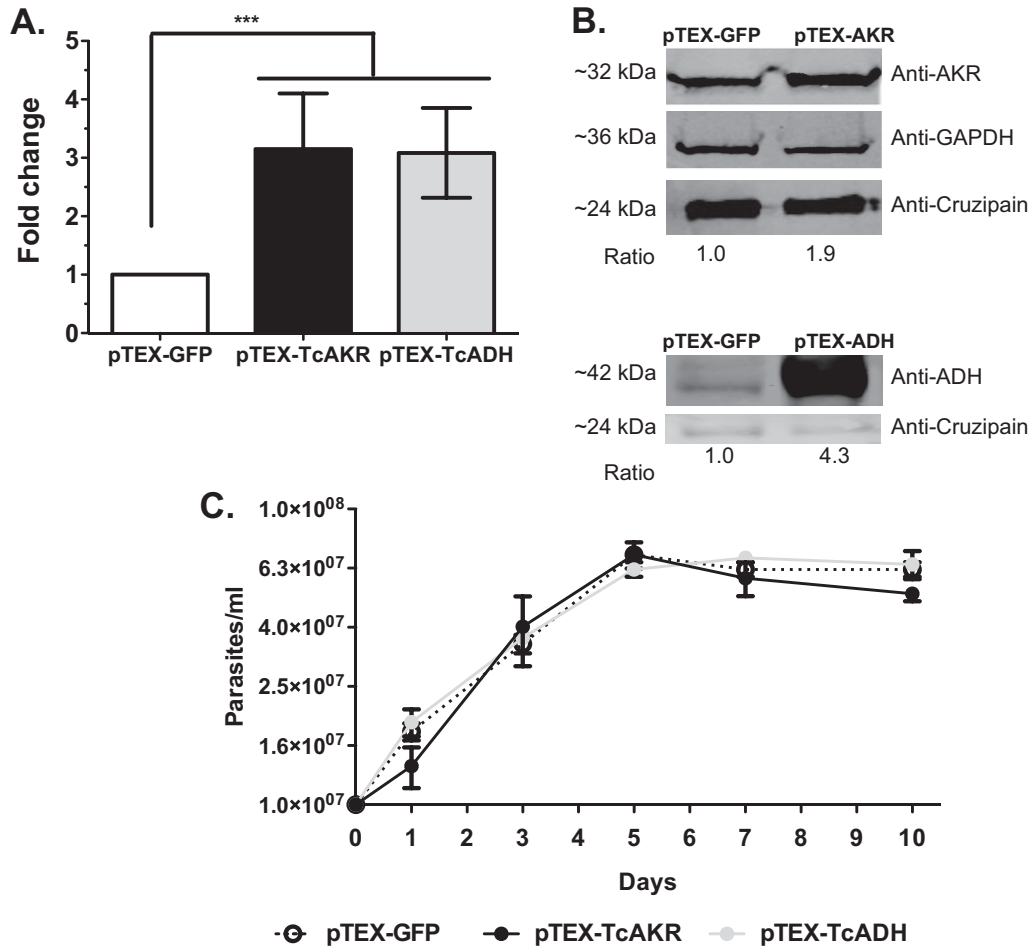


Fig. 2. Biological and molecular characterization of *T. cruzi* pTEX-GFP (white), pTEX-TcAKR (black) and pTEX-TcADH (gray) transfected parasites. *T. cruzi* 61S clone was transfected with pTEX-GFP, pTEX-TcAKR and pTEX-TcADH and different experiments were performed to characterize the overexpression.

A. qRT-PCR to quantify the mRNA levels of the *AKR* and *ADH* genes in the transfected parasites. The mRNA levels were normalized using the expression of two reference genes (HGPRT and 24S alpha ribosomal RNA). The relative quantification results were obtained using the REST2009 program by a randomization test with 10,000 permutations ($P < 0.05$). The graph shows the data of each gene evaluated for each of the overexpressing phenotypes compared with pTEX-GFP parasites (white bars represent pTEX-GFP parasites; black bars correspond to pTEX-TcAKR; gray bars represent pTEX-TcADH phenotype) in triplicate and two independent experiments. * $P < 0.05$; ** $P < 0.01$; *** $P < 0.001$.

B. Analysis of TcAKR and TcADH proteins expression by Western blotting in epimastigotes of the *T. cruzi* pTEX-GFP, pTEX-TcAKR and pTEX-TcADH transfected parasites using mouse anti-rTcAKR polyclonal serum (1:500) and rabbit anti-rTcADH polyclonal serum (1:500) respectively, with rabbit anti-cruzipain polyclonal serum (1:500), and mouse anti-GAPDH polyclonal serum (1:300) as a loading control. The numbers in the bottom of the membranes correspond to the fold of expression compared with the loading controls and analyzed by densitometry using the ImageJ software.

C. Cumulative cell density of pTEX-GFP (white), pTEX-TcAKR (black) and pTEX-TcADH (gray) transfected parasites counted every two days for 10 days by triplicate.

control at 96 h and more obvious after seven days (Fig. 4A). Similar results were obtained with the GO treatment, since that pTEX-TcAKR and pTEX-TcADH parasites presented a significant increase ($P < 0.001$) in cell viability when compared with the control, keeping 90% of viable parasites, even until 96 hours, at which time there was only less than 10% of viable pTEX-GFP parasites (Fig. 4B). There were not changes in the cell viability through time of the untreated parasites.

Overexpression of TcAKR and TcADH counteracts the mitochondrial and cell membrane damaged after the treatment with Bz and GO

At 72 and 96 h between the 6 and 10% of pTEX-GFP parasites treated with Bz showed a decrease in the mitochondrial membrane potential. Likewise, the cell membrane damage increased significantly in the same population at 96 h. Conversely, parasites overexpressing TcAKR and TcADH presented significant ($P < 0.01$) less damage in these parameters when compared with the

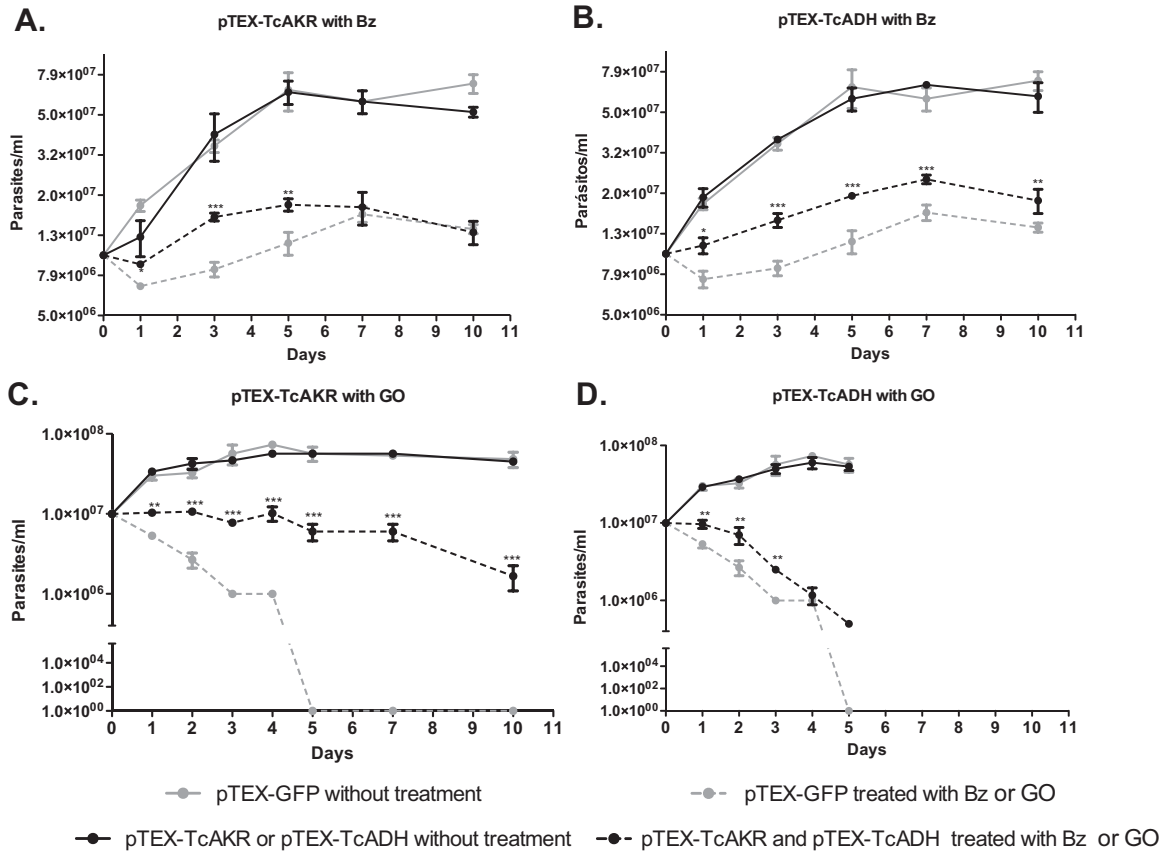


Fig. 3. Growth curves in presence of Bz and GO of pTEX-TcAKR and pTEX-TcADH parasites. Treated (dashed lines) and untreated parasites (continuous lines) were followed during 10 days by microscope counting. A and B. pTEX-TcAKR and pTEX-TcADH parasites respectively, treated with 60 μ M Bz and compared with the control (pTEX-GFP). C and D. pTEX-TcAKR and pTEX-TcADH parasites respectively, treated with GO 30 mM and compared with the control (pTEX-GFP). Experiments were performed in triplicate, with data presented as the means \pm SD. For statistically significant ANOVA was used and t-test to compare sample means from two independent groups. * $P < 0.05$; ** $P < 0.01$; *** $P < 0.001$.

control (Fig. 4C and E). Notably at 168 h, there were not significant differences in these parameters between transfected parasites and the control, but at this time around 40% of the control parasites were death (Fig. 4A). After GO treatment, we observed that the viability loss with this compound is mainly due to damage of the cell membrane since at 72 and 96 h between 50 and 90% of the parasites showed a damage in this structure (Fig. 4D and F) and that the overexpression of both genes, as was observed with Bz, decreased significantly ($P < 0.001$) these effects, conferring protection specially against cell membrane damage (Fig. 4F).

TcAKR and TcADH are involved in the detoxification of ROS, which increases the cell infectivity

In order to evaluate the role of these genes in ROS detoxification, we measured the intracellular ROS concentration in the pTEX-GFP and transfected parasites after treatment with Bz or GO. The ROS level in pTEX-

TcAKR and pTEX-TcADH parasites at 72 h after Bz treatment decreased significantly ($P < 0.001$) with respect to the control and non-treated transfected parasites (Fig. 5A). In addition, at 24 h after treatment with GO, similar results were found (data not shown). Interestingly, when we quantified the pTEX-TcAKR and pTEX-TcADH infectivity in VERO cells and the number of intracellular amastigotes as a feature related to the ROS levels, these parasites were more infective ($P < 0.001$) than the control (Fig. 5B).

Discussion

In this work, we used two clones isolated from a *T. cruzi* strain that was previously classified as Bz-resistant (Mejía-Jaramillo *et al.*, 2012). Interestingly, these two clones showed different EC_{50} to Bz but similar genetic backgrounds and slight differences in some biological features. This result is very important because it indicates that the multiclonality of *T. cruzi* could affect the

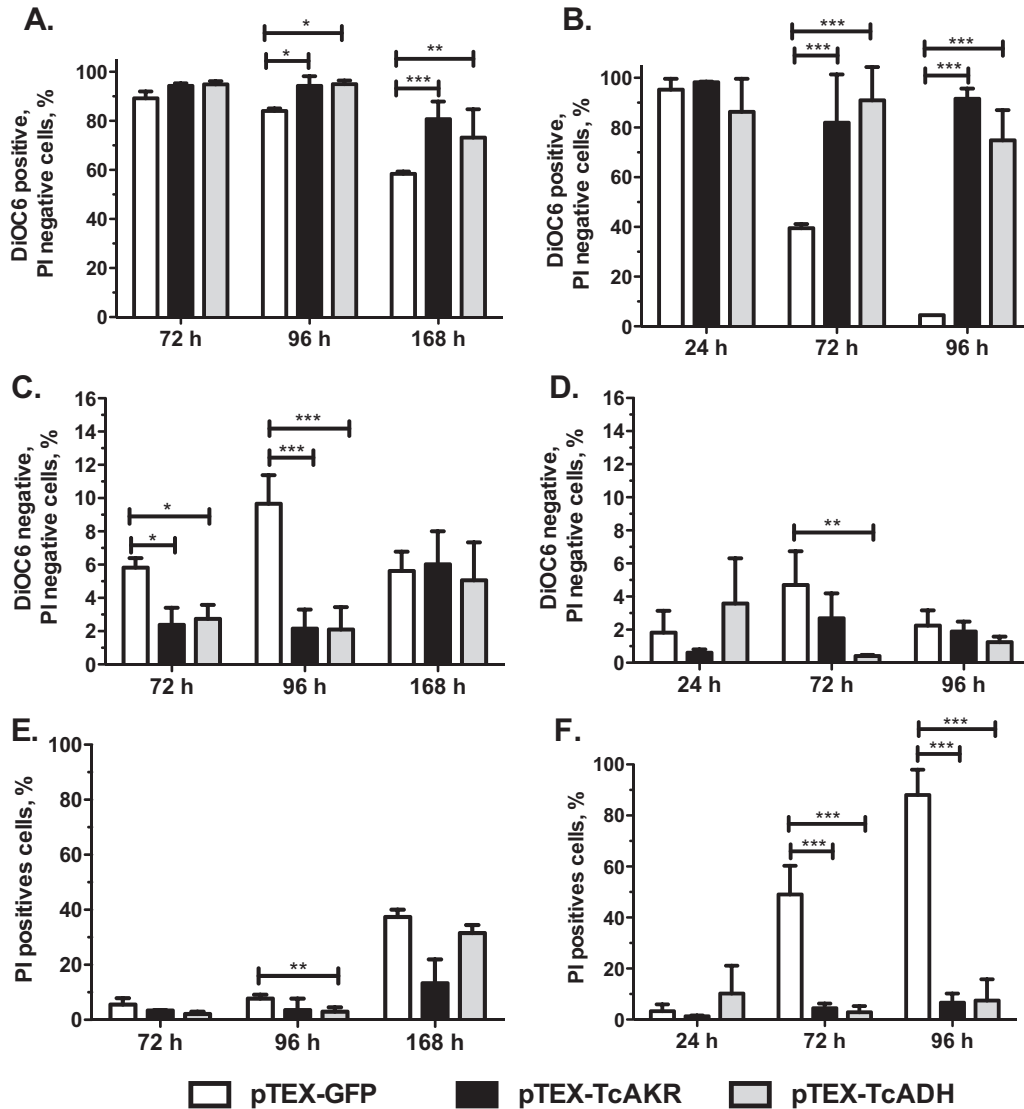


Fig. 4. Effect of Bz and GO on the cell viability, mitochondrial potential and cell membrane damage in pTEX-GFP, pTEX-TcAKR and pTEX-TcADH transfected parasites.

A and B. Percentage of viable cells after treatment with Bz and GO respectively. The results correspond to the percentage of DiOC6-positive and PI-negative cells quantified by flow cytometry.

C and D. Mitochondrial potential damage of treated cells with Bz and GO respectively. The results correspond to the percentage of DiOC6-negative and PI-negative cells quantified by flow cytometry. pTEX-TcAKR and pTEX-TcADH parasites presented less damage than control parasites.

E and F. Cell membrane damage of treated cells with Bz and GO respectively. The results correspond to the percentage of PI-positive and DiOC6-positive quantified by flow cytometry. Transfected parasites presented less damage in the membrane due to the less % of positive PI cells. Experiments were performed in triplicate, with data presented as the means \pm SD. * $P < 0.05$; ** $P < 0.01$; *** $P < 0.001$. In all experiments Bz, (60 μ M) and GO (30 mM) were used at three different times; pTEX-GFP (white), pTEX-TcAKR (black) and pTEX-TcADH (gray).

treatment due to the presence of resistant clones in the strains (Tibayrenc *et al.*, 1986; Filardi and Brener, 1987). Although the resistant clone has a decreased cell infectivity, under treatment, it could survive and persist in the host, causing a treatment failure (Filardi and Brener, 1987; Hayes and Wolf, 1990). This finding was corroborated by assessing the susceptibility to Bz in amastigotes and trypomastigotes showing that the DA-R

clone is more resistant to the treatment with the drug compared to DA-S clone in all parasitic stages.

In the context of these two clones having different EC_{50} , we thought that finding some differentially expressed proteins by 2D-gels could explain the differences in response to Bz. Several studies have shown that one of the ways to gain a resistant phenotype is by changing the expression of important proteins that are

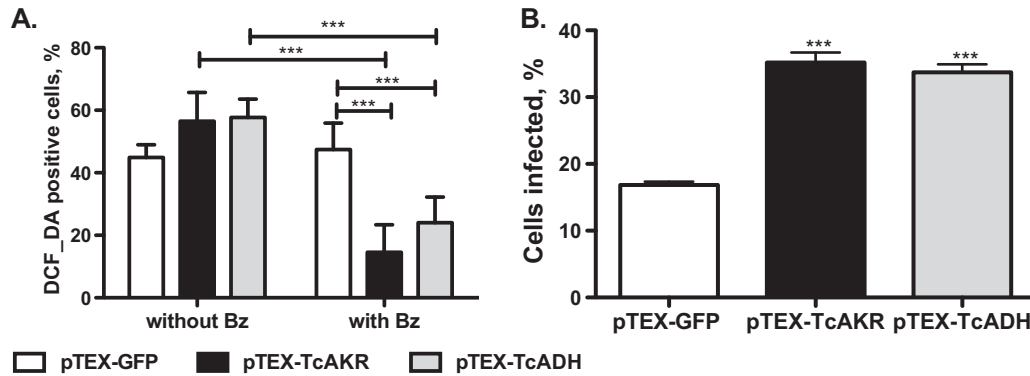


Fig. 5. Levels of intracellular ROS in pTEX-GFP (control), pTEX-TcAKR (black) and pTEX-TcADH (gray). A. Intracellular ROS quantification with and without Bz (60 μ M) treatment after 72 h. The results correspond to the percentage of DCF-DA-positive cells quantified by flow cytometry. B. Infection of VERO cells stained with Giemsa, as explained in Figure 1B.

involved in the activation of drugs, detoxification, DNA repair or membrane transporters (Hayes and Wolf, 1990). In our study, we found that 28% of the analyzed proteins were unique or overexpressed and that they could be involved in the resistance to drugs. Other studies that used resistant clones obtained by *in vitro*-induced resistance to Bz using increased pressure of drug found a greater number of proteins, approximately 65% (Andrade *et al.*, 2008). However, this result may be explained by different Bz EC_{50} values of these two resistant clones analyzed (50 μ M vs. 220 μ M), as well as the processes to achieve the resistance, as was observed in our biological annotation data, which included genes mainly associated with purine metabolism.

Since many of the proteins selected in our study, seemed to not have a direct role in resistance to Bz, and many of those likely involved in resistance have been studied previously, the TcAKR and TcADH proteins caught our attention. Both proteins were overexpressed in the resistant clone, and have been associated with biotransformation reactions type II in organisms such as yeast, *Escherichia coli* and mammals. In this process oxidation-reduction reactions can lead to the final detoxification of xenobiotics (Bakker *et al.*, 2000; Macherey and Dansette, 2008; Parkinson *et al.*, 2013; Penning, 2014a, 2014b), ROS (Shangari and O'Brien, 2004; Shangari *et al.*, 2006; Li and Ellis, 2014) and endogenous metabolites such as carbonyl adducts, glyoxal and methyl glyoxal (Shangari and O'Brien, 2004; Hoon *et al.*, 2011; Lee *et al.*, 2013).

As mentioned previously, one of the main mechanisms of drug resistance is the over or down expression of important proteins, a phenomenon that can be achieved by gene amplification or deletion, point mutation and positive or negative mRNA posttranscriptional regulation (Hayes and Wolf, 1990; Blanchard, 1996;

Upcroft and Upcroft, 2001; Tenover, 2006; Andrade *et al.*, 2008). In this sense, we compared the sequence from TcAKR and TcADH genes in sensitive and resistant parasites and no changes in the nucleotide or amino acid sequences that could explain the different phenotypes were found. Consistent with the results obtained by 2D-gels, we decided to evaluate if changes in the levels of TcAKR and TcADH could be associated with the resistant phenotype. To accomplish this, we overexpressed these genes in sensitive parasites and we determine how they could be involved in the generation of the Bz resistance phenotype in *T. cruzi*.

In this sense, we found that the overexpression of both genes leads to an increased survival percentage after treatment with Bz and GO compounds. Bz produces, by action of NTR I (Hall and Wilkinson, 2012), GO, which in turn forms adducts with nucleotides and leads to DNA mutations (Kasai *et al.*, 1998; Chen and Hu, 2009; Bot *et al.*, 2010); additionally, by protein glycation, GO inhibits thioredoxin reductase, glutathione reductase, superoxide dismutase and some dehydrogenases, reducing oxidative defense (Shangari *et al.*, 2003, 2006). In the same way, the activation of Bz increases the concentration of intracellular ROS, either due to the Bz-induced increase of ROS per se or by depletion of the detoxification enzymes, causing mutations and DNA damage (Pedrosa *et al.*, 2001; Furtado *et al.*, 2014). In addition, Bz induces the arrest of cells in the M control site, as has been shown for cell lines such as HeLa, RAW 264.7 and THP-1 (Pascutti *et al.*, 2009; Calvo *et al.*, 2013), allowing the DNA damage repair or trigger cell death to proceed (Boonstra and Post, 2004; Verbon *et al.*, 2012). In this sense, the increased viability of the parasites in the presence (Fig. 3) of Bz and GO and the decrease of intracellular ROS found in parasites overexpressing TcAKR could be due to its role as a detoxifying enzyme, which was recently

demonstrated (Garavaglia *et al.*, 2016) and also confirmed in this study. Studies on the carbonyl stress performed in bacteria showed that *E. coli* AKR (YafB, YqhE, YeaE and YghZ) with aldehyde reductase (YqhD) is actively involved in the detoxification of toxic compounds such as GO and methyl-glyoxal (Kwon *et al.*, 2012; Lee *et al.*, 2013), which accumulate in the cells due to endogenous metabolism as a result of the protein glycation, lipid peroxidation, DNA oxidation and autoxidation of sugars (Ahmed *et al.*, 2011; Lange *et al.*, 2012). Additionally, in humans, overexpression of AKRs restores the levels of glutathione, a major endogenous antioxidant, which is lost by exposure to GO, leading to an increased peroxide resistance and a decreased rate of mutations (Shangari and O'Brien, 2004; Barski *et al.*, 2008; Penning, 2014a, 2014b). Thus, in *T. cruzi*, it is probable that AKR leads to the formation of ethylene glycol (1,2-Ethandiol) from GO, avoiding the inhibition of the antioxidant enzymes and maintaining normal glutathione levels, which results in a decrease of GO-nucleotide adducts and less ROS stress (Kwon *et al.*, 2012) (Fig. 5).

On the other hand, the overexpression of TcADH allows viable cultures to have more time when they are exposed to Bz and GO by decreasing the percentage of parasites with damage in the plasma membrane (Fig. 4), and showing that this overexpression is able to detoxify GO as it does in *Saccharomyces cerevisiae* (Hoon *et al.*, 2011; Kwon *et al.*, 2012). In yeast, the ADH6 deletion increased sensitivity to GO (Hoon *et al.*, 2011), although the molecular mechanisms by which this response is given have not been explained, there is strong evidence indicating an interaction between GO with ADH residues such as lysine and arginine, leading to the inhibition of ADH (Jörnvall, 1970; Canella and Sodini, 1975), which in turn manages the intracellular concentration of GO, preventing the inhibition of other detoxifying enzymes and avoiding adduct formation. Similarly, the evidence found in other organisms indicated that ADH has a protective effect against the oxidative stress caused by hydrogen peroxide (H₂O₂) (Fig. 5). In *E. coli*, mutants with a deletion of adhE showed increased sensitivity to this compound. Echave *et al.* showed that peroxide reacts with the enzyme ADH *in vitro* and *in vivo*, which leads to irreversible inactivation of the enzyme and peroxide homeostasis under normal aerobic conditions (Echave *et al.*, 2003). This finding could explain the similar ROS levels that were found between pTEX-ADH and pTEX-GFP several hours post-treatment.

We found that TcAKR and TcADH overexpression does not have a biological cost as has been shown in several organisms; in fact, their overexpression increased the infectivity rate due probably to the

resistance to oxidative stress (Ughes and Andersson, 1998; Villarreal *et al.*, 2005; Andersson, 2006; Wilkinson *et al.*, 2008; Sandegren *et al.*, 2008; Mejía *et al.*, 2012). Interestingly, the results obtained in this work are indicating that during first 72 h of treatment, Bz affect the mitochondrial membrane potential but the viability is not altered (Fig. 4A–C). At 96 h the parasites are showing additionally damage at cell membrane level, which finally affect their survival but the overexpression of these genes counteract significantly these effects.

Finally, we propose that resistance to Bz in *T. cruzi* is a multigenic trait, where other enzymes besides NTR I are participating, such as TcAKR and TcADH. The specific role of these proteins should be studied in future works, but we hypothesize based in our results and other report in *T. cruzi* and different organism, that Bz is activated by the action of NTR I to form GO (Hall and Wilkinson, 2012) or by other nitroreductases to produce ROS (Pedrosa *et al.*, 2001; Furtado *et al.*, 2014). The TcAKR enzyme is able to reduce Bz using NADPH as co-factor (Garavaglia *et al.*, 2016) and together with other enzymes transforms GO in 1,2-Ethandiol (Kwon *et al.*, 2012; Lee *et al.*, 2013) and detoxifies ROS (Ahmed *et al.*, 2011; Li *et al.*, 2012). TcADH detoxifies GO (Hoon *et al.*, 2011) and is capable of binding irreversibly to H₂O₂, decreasing the ROS intracellular concentration (Echave *et al.*, 2003). The reduction of GO and ROS concentrations by TcAKR and TcADH decreases the toxic effects caused by these compounds: inhibition of enzymes (Shangari *et al.*, 2003), glutathione (GSH) decrease and nucleotide adducts, which forms mutations and DNA lesions (Chen and Chen, 2009) and leads to cell arrest or cell death (Boonstra and Post, 2004; Larsen *et al.*, 2012; Verbon *et al.*, 2012) (Fig. 6). Thus, parasites with increased expression of these enzymes could gain resistance or tolerance to Bz. However, it remains to be elucidated whether Bz reduction by TcAKR can favor per se the resistance to Bz or the resistance is the result of the other putative activities of this enzyme.

In summary, we found that the overexpression of the *TcAKR* and *TcADH* genes enhances the resistance to Bz and GO, which was supported by increasing the survival and the EC₅₀ to Bz and by decreasing the mitochondrial and cell membrane damage and the concentrations of intracellular ROS after the treatment with both compounds, providing evidence that both genes may have an important role in the resistance to Bz. Thus, in the near future, it could be proposed that the *TcADH* and *TcAKR* genes will be candidates for biomarkers of natural resistance, detectable before or during treatment, increasing the likelihood of success of chemotherapeutics, which will allow combination

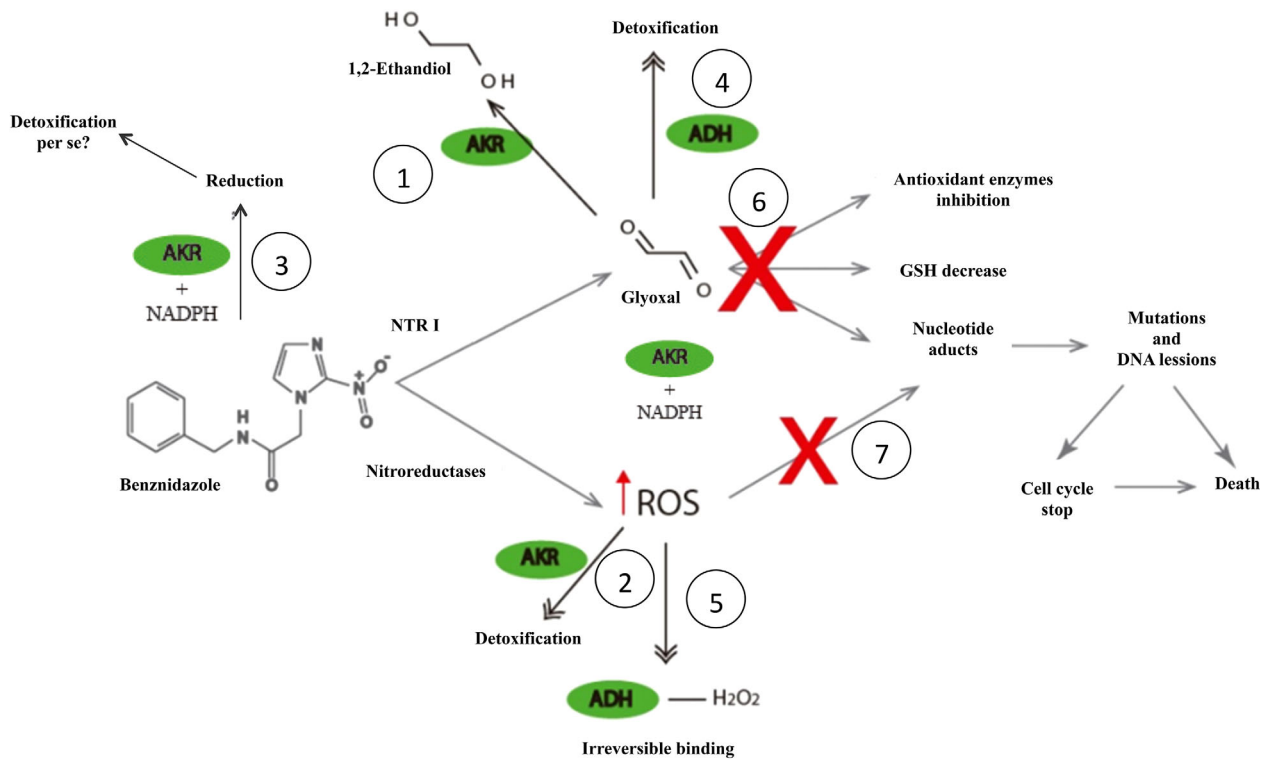


Fig. 6. Model of the role of AKR and ADH enzymes in the resistance to Bz. Bz is activated by the action of NTR I to form glyoxal or by other nitroreductases to produce ROS. The AKR enzyme together with other enzymes may transform glyoxal to 1,2-ethandiol (1), could detoxify ROS (2) and is able to reduce Bz using NADPH as co-factor (3). ADH could detoxify glyoxal and ROS (4), and might be able of binding irreversibly to H₂O₂, decreasing the ROS intracellular concentration (5). The reduction of glyoxal (6) and ROS (7) concentrations by AKR and ADH should decrease the toxic effects caused by these compounds: inhibition of enzymes, decrease of glutathione (GSH), and decrease of nucleotide adducts, which forms mutations and DNA lesions and leads to cell arrest or cell death.

therapies of Bz or Nfx with inhibitors of these detoxifying enzymes, such as disulfiram (Carper *et al.*, 1987).

Experimental procedures

Strains and clones

The DA strain, donated by National Institute of Health from Colombia (INS), was isolated by blood culture from a two-year-old child in the acute phase of *T. cruzi* infection. This strain was characterized as *T. cruzi* I (MHOM/CO/2001/DA), and the epimastigotes have an effective concentration 50 (EC₅₀) to Bz of 32.8 μM (Mejía *et al.*, 2012). Clones from this strain were obtained using the single cell cycling mode of a cell sorter MOFLO XDP (Beckman Coulter, Indianapolis, IN, USA) with 97% performance success. For transfections, the 61S clone also characterized as *T. cruzi* I (M.RATTUS/CO/91/GAL-61cl11), and with EC₅₀ to Bz of 11 μM by MTT assay was used.

Cultures

T. cruzi epimastigotes were cultivated in supplemented Roswell Park Memorial Institute (RPMI) 1640 medium at

28°C. Transformed *T. cruzi* were maintained with 100 μg ml⁻¹ of Geneticin (G418). Wild type and transfected parasite growth curves were started at 1 × 10⁶ and 1 × 10⁷ cells ml⁻¹ respectively, and the cells were counted for 10 days. Amastigotes were grown in African green monkey kidney (VERO) cells cultured in DMEM/2% FBS at 37°C in 5% CO₂. To generate metacyclic trypomastigotes, epimastigote cultures were grown to the stationary phase, at which point they differentiated. These were used to infect monolayers at a ratio of nine metacyclics per mammalian cell. Following overnight incubation at 37°C, extracellular metacyclics and epimastigotes were removed by several washes. Metacyclic trypomastigotes emerged between day 7 and 10, and this homogeneous population was used in the quantitative infection experiments.

Determination of susceptibility to Bz in different parasite stages

To determine the susceptibility to Bz of epimastigotes, amastigotes and trypomastigotes, different methodologies, according to the conditions growth of each state, were used. Thus, a total of 2 × 10⁶ epimastigotes ml⁻¹ were cultured with eleven concentrations of Bz (0–400 μM) by triplicate for 72 h at 28°C in 96-well microtiter plates. The plates

were then incubated with 5 mg ml⁻¹ 3-(4,5-dimethylthiazol-2-yl)-2,5-diphenyltetrazolium bromide (MTT) for 90 min, and MTT reduced to formazan crystals was measured at 595 nm. Amastigote susceptibility was calculated by infecting 30,000 VERO cells per well with 5 trypomastigotes per cell in 24-well microplates with rounded coverslips on the bottom. Attachment and invasion were allowed for 24 h and then the medium was removed and washed three times with PBS 1X to eliminate non-infecting trypanosomes. Bz was added at different concentrations (0–100 µM) in fresh medium and after 48 h, the coverslips were fixed and stained with Giemsa. The number of amastigotes in 200 cells were counted in each treatment. Finally, 1 × 10⁶ trypomastigote forms obtained from VERO cells were incubated at 37°C in DMEM medium without FBS with different concentrations (0–100 µM) of Bz in 24-well plates and counted after 24 h. All experiments were performed in duplicate or triplicate, and results were expressed as means ± standard deviations (SD).

Genotyping of *T. cruzi* clones and characterization of NTR I gene

To select two clones from the original strain with a different susceptibility to Bz but with similar genetic background, the random amplification of polymorphic DNA (RAPD) and low-stringency single specific primer PCR (LSSP-PCR) profiles from the minicircles variable region (kDNA) and the intergenic regions of the spliced-leader mini-exon genes (SL-mini-exon) were used as described before (Steindel *et al.*, 1994; Mejía-Jaramillo *et al.*, 2009; Rodríguez *et al.*, 2009). All of the amplification products were analyzed in 8% polyacrylamide gels and visualized with silver staining.

Additionally, the *NTR I* gene from the two selected clones was amplified and sequenced (Mejía *et al.*, 2012). Each sequence was aligned using the ClustalX program and compared to the sequence of the *NTR I* gene from the DA strain, one sensitive (61S) and three resistant clones obtained by drug pressure (61R-3, 61R-4 and 61R-6), which were previously reported by Mejía *et al.* (Mejía *et al.*, 2012). Additionally, the mRNA levels of the *NTR I* gene were quantified by qRT-PCR as previously described (Mejía-Jaramillo *et al.*, 2011) and compared between the sensitive and resistant clones.

Proteome analysis

Protein extracts were obtained from 20 ml of exponential growth epimastigotes culture (1 × 10⁷ parasites ml⁻¹) from sensitive and resistant clones, which were performed in triplicate. Parasites were harvested by centrifugation and washed with PBS (pH 7.2) and hypotonic PBS (13.6 mM NaCl, 0.27 mM KCl, 0.4 mM Na₂HPO₄, 0.15 mM K₂HPO₄) with 1X protease inhibitor (Complete, EDTA-free protease inhibitor cocktail tablets, Roche). The parasites were lysed by 15 cycles of 5 min of sonication on ice and 1 min of liquid nitrogen freezing. The soluble fraction was obtained by centrifugation and washed with cold acetone. The pellet was suspended in isoelectric focusing buffer, incubated for 24 h at 4°C and sonicated (10 cycles). The protein

concentration was determined using a 2D QUANT kit (GE Healthcare Life Sciences, Pittsburgh, PA, USA).

For the first dimension, proteins were separated on polyacrylamide strips of immobilized pH gradient (IPG) of 7 cm long, with a pH range of 5–8 (GE Healthcare Life Sciences, Pittsburgh, PA, USA) using an Ettan IPGphor 3 system. Passive rehydration was performed for 12 h. After IEF, the strips were incubated for 15 min in equilibrium buffer I, followed by a second incubation step in equilibrium buffer II (iodoacetamide 25 mg ml⁻¹). The IPG strips were placed into a 12% polyacrylamide gel and run in a Mini-PROTEOMETER Tetra Cell with Tris/Glycine/SDS buffer, using 20 V cm⁻¹ for 120 min, and then stained with Coomassie blue G-250.

2-DE image analysis and protein identification

Gels were digitalized in an ImageScannerTM III (GE Healthcare Life Sciences, Pittsburgh, PA, USA), and differential image analysis was performed in the ImageMaster 2D Platinum 7.0 software (GE Healthcare Life Sciences, Pittsburgh, PA, USA). For each clone, three independent gels were made. The parameters used for spot selection were: smooth 2, saliency 24, and minimum area 1. Each spot was validated by visual inspection and edited when necessary. The intensity of each protein spot was normalized relative to the total intensity of all valid spots. After normalization and background subtraction, a matched set was created and the differential expression analysis was performed, comparing the quantity of the matched spots in sensitive and resistant clones. The cut-off limit employed was based on a *P* value of ≤ 0.05.

The selected spots were excised from the gel and sent to the Mass Spectrometry Laboratory in Texas, US for the sequence identification by MALDI-TOF/TOF technique. The identification was made by the Matrix Science Mascot program (<http://www.matrixscience.com/>), and the functional annotation was performed with the TriTryp database (<http://www.tritrypdb.org/tritrypdb/>). Finally, the functional annotation was assigned using Blast2GO (Conesa and Götts, 2008).

Overexpression of *TcAKR* and *TcADH*

To overexpress active protein in sensitive 61S *T. cruzi* parasites, the full-length *TcAKR* (849 bp) and *TcADH* (1179 bp) genes were amplified from a sensitive clone DNA and ligated into the XbaI/XhoI and HindIII/XhoI sites respectively, of the vector pTEX (Kelly *et al.*, 1992). The constructs were confirmed by sequencing. Epimastigotes from 61S clone were electroporated, and transformants were selected with 100 µg ml⁻¹ G418. *TcAKR* and *TcADH* mRNA levels were verified by qRT-PCR using the specific primers *TcAKR* (F-5'-CTACCGCCACATCGACAC-3' R-5'-TTGTTACCCACACCTCC TCA-3') and *TcADH* (F-5'-TAACGCTATCCTGCTGCCAC-3' and R-5'-TCATCCATGCCCGTCGTACT-3') following conditions described by Mejía *et al.* (Mejía-Jaramillo *et al.*, 2011); and by northern blot analysis, according to the conditions previously described by Kim *et al.* (2010), with minor adjustments (Kim *et al.*, 2010). Moreover, the overexpression was confirmed by western blot using anti-*TcAKR* and anti-*TcADH*

polyclonal antibodies prepared in mouse and rabbits respectively, as have been described in (Campos *et al.*, 2009; Garavaglia *et al.*, 2016) and using GADPH or/and cruzipain as load control prepared in mouse and rabbit respectively. 61S parasites transfected with pTEX-GFP were used as a control.

Sensitivity experiments to Bz and GO

To evaluate the response to Bz, the MTT assay was used as described above and the EC₅₀ was calculated. For GO (one by-product of Bz), the EC₅₀ was determined by exposing the transfected parasites to a range of concentrations (5, 10, 20, 30, 40 mM) for 24 h. The cell numbers were determined in a cytometry chamber using the erythrosine-b vital stain to differentiate living and dead cells. The results were expressed as the survival growth percentage compared to untreated cultures. In both cases, the experiments were performed by triplicate in two independent experiments. Finally, the growth kinetics of transfected parasites treated with both drugs was followed during 10 days after the treatment with 60 μM Bz or 30 mM GO to evaluate the effect of the overexpression of these genes in the survival of parasites through time. All the experiments were performed in triplicate.

Cell viability, mitochondrial membrane potential, cell membrane damage and intracellular ROS quantification by flow cytometry

Flow cytometry experiments were performed in a BD FACS-Canto II machine (BD Biosciences, San Jose, CA, USA). In total, 10,000 events were acquired in the regions previously identified as corresponding to *T. cruzi* epimastigotes. The data were analyzed with FlowJo software (Treestar software). All experiments were performed at least in triplicate.

1×10^7 parasites ml⁻¹ in the exponential phase were treated with Bz (60 μM) or GO (30 mM) and analyzed at different times. For cell viability, mitochondrial membrane potential and cell membrane damage analysis, parasites were counted and diluted to a final concentration of 1×10^6 parasites ml⁻¹ in fresh medium, and resuspended in 20 μg ml⁻¹ propidium iodide (PI) and 0.4 μg ml⁻¹ 3,3'-dihexyloxycarbocyanine iodide (DiOC6) and immediately quantified, without washing by flow cytometry. DiOC6-positive and PI-negative cells were considered to be alive, DiOC6-negative and PI-negative cells have mitochondrial potential damage and DiOC6-positive and PI-positive cells were quantified as cells with membrane damage.

For intracellular ROS quantification, 1×10^6 parasites were incubated for 5 min at 28°C with 0.1 μM H₂DCFDA probe, washed three times in PBS and immediately quantified by flow cytometry. The mean fluorescence intensity, which is an indirect measure of the concentration of intracellular ROS, was measured in the positive DCF-DA parasite population.

Statistical analysis

To examine if the data were normally distributed, a Kolmogorov–Smirnov test was used. Once the parametric assumption was satisfied, a two-way ANOVA was used to

compare the independent groups. For statistically significant ANOVA outcomes, the independent samples t-test was used to compare sample means from two independent groups. Bonferroni corrections for multiple comparisons were performed.

Acknowledgements

We are particularly grateful to Professor Mauricio Rojas for his help in the flow cytometry experiments and analyses and to the INS for providing the DA strain. This research was supported by the Universidad de Antioquia (UdeA) and COLCIENCIAS (Project number 111551929168). PGH and LG were supported by fellowship from COLCIENCIAS and SMFM by CNPq/Brasil. The authors declare that they have no conflict of interests.

Authors' contributions

AMMJ and OTC conceived the study and participated in its design and coordination. LG, PGH, SMFM and GAG performed the experiments. AMMJ and OTC wrote the manuscript, and all authors read and approved the final manuscript.

References

- Ahmed, M.M.E., Wang, T., Luo, Y., Ye, S., Wu, Q., Guo, Z., *et al.* (2011) Aldo-keto reductase-7A protects liver cells and tissues from acetaminophen-induced oxidative stress and hepatotoxicity. *Hepatology* **54**: 1322–1332.
- Andersson, D.I. (2006) The biological cost of mutational antibiotic resistance: any practical conclusions? *Curr Opin Microbiol* **9**: 461–465.
- Andrade, H., Murta, S.M.F., Chapeaurouge, A., Perales, J., Nirdé, P., and Romanha, A.J. (2008) Proteomic Analysis of *Trypanosoma cruzi* resistance to benznidazole. *J Proteome Res* **7**: 2357–2367.
- Apt, W., and Zulantay, I. (2011) Estado actual en el tratamiento de la enfermedad de Chagas. *Rev Med Chil* **139**: 247–257.
- Bakker, B.M., Bro, C., Kotter, P., Luttk, M.A.H., Dijken, J.P., Van., and Pronk, J.T. (2000) The mitochondrial alcohol dehydrogenase ADH3p is involved in a redox shuttle in *Saccharomyces cerevisiae*. *J Bacteriol* **182**: 4730–4737.
- Barski, O.A., Tipparaju, S.M., and Bhatnagar, A. (2008) The aldo-keto reductase superfamily and its role in drug metabolism and detoxification. *Drug Metab Rev* **40**: 553–624.
- Blanchard, J.S. (1996) Molecular mechanisms of drug resistance in *Mycobacterium tuberculosis*. *Annu Rev Biochem* **65**: 215–239.
- Boonstra, J., and Post, J.A. (2004) Molecular events associated with reactive oxygen species and cell cycle progression in mammalian cells. *Gene* **337**: 1–13.
- Bot, C., Hall, B.S., Bashir, N., Taylor, M.C., Helsby, N. A., and Wilkinson, S.R. (2010) Trypanocidal activity of

- aziridinyl nitrobenzamide prodrugs. *Antimicrob Agents Chemother* **54**: 4246–4252.
- Calvo, K.L., Ronco, M.T., Noguera, N.I., and García, F. (2013) Benzimidazole modulates cell proliferation in acute leukemia cells. *Immunopharmacol Immunotoxicol* **35**: 478–486.
- Campos, F.M.F., Liarte, D.B., Mortara, R. A., Romanha, A.J., and Murta, S.M.F. (2009) Characterization of a gene encoding alcohol dehydrogenase in benzimidazole-susceptible and -resistant populations of *Trypanosoma cruzi*. *Acta Trop* **111**: 56–63.
- Campos, M.C.O., Leon, L.L., Taylor, M.C., and Kelly, J.M. (2014) Benzimidazole-resistance in *Trypanosoma cruzi*: Evidence that distinct mechanisms can act in concert. *Mol Biochem Parasitol* **193**: 17–19.
- Cançado, J.R. (1999) Criteria of Chagas disease cure. *Mem Inst Oswaldo Cruz* **94**: 331–335.
- Canella, M., and Sodini, G. (1975) The reaction of horse-liver alcohol dehydrogenase with glyoxal. *Eur J Biochem* **59**: 119–125.
- Carper, W.R., Dorey, R.C., and Beber, J.H. (1987) Inhibitory effect of disulfiram (Antabuse) on alcohol dehydrogenase activity. *Clin Chem* **33**: 1906–1908.
- Chen, H.-J.C., and Chen, Y.-C. (2009) Analysis of glyoxal-induced DNA cross-links by capillary liquid chromatography nanospray ionization tandem mass spectrometry. *Chem Res Toxicol* **22**: 1334–1341.
- Chen, Y., and Hu, L. (2009) Design of anticancer prodrugs for reductive activation. *Med Res Rev* **29**: 29–64.
- Conesa, A., and Götz, S. (2008) Blast2GO: A comprehensive suite for functional analysis in plant genomics. *Int J Plant Genomics* **2008**: 619832.
- Coronado, X., Zulantay, I., Rozas, M., Apt, W., Sánchez, G., Rodríguez, J., *et al.* (2006) Dissimilar distribution of *Trypanosoma cruzi* clones in humans after chemotherapy with allopurinol and itraconazole. *J Antimicrob Chemother* **58**: 216–219.
- Coura Rodriguez, J. and de Castro, S.L. (2002) A critical review on Chagas disease chemotherapy. *Mem Inst Oswaldo Cruz* **97**: 3–24.
- Echave, P., Tamarit, J., Cabisco, E., and Ros, J. (2003) Novel antioxidant role of alcohol dehydrogenase E from *Escherichia coli*. *J Biol Chem* **278**: 30193–30198.
- Filardi, L.S., and Brener, Z. (1987) Susceptibility and natural resistance of *Trypanosoma cruzi* strains to drugs used clinically in Chagas disease. *Trans R Soc Trop Med Hyg* **81**: 755–759.
- Furtado, C., Alves, C.L., Passos-Silva, D.G., Moura, M.B., De, Schamber-Reis, B.L., Kunrath-Lima, M., *et al.* (2014) Unveiling Benzimidazole's mechanism of action through overexpression of DNA repair proteins in *Trypanosoma cruzi*. *Environ Mol Mutagen* **55**: 309–321.
- Garavaglia, P.A., Garcia, G.A., Laverriere, M., and Cannata, J.J.B. (2016) Putative role of the aldo-keto reductase from *Trypanosoma cruzi* (TcAKR) in benzimidazole metabolism. *Antimicrob Agents Chemother* **60**: 2664–2670.
- Hall, B.S., and Wilkinson, S.R. (2012) Activation of benzimidazole by trypanosomal type I nitroreductases results in glyoxal formation. *Antimicrob Agents Chemother* **56**: 115–123.
- Hayes, J.D., and Wolf, C.R. (1990) Molecular mechanisms of drug resistance. *Biochem J* **272**: 281–295.
- Hoon, S., Gebbia, M., Costanzo, M., Davis, R.W., Giaever, G., and Nislow, C. (2011) A global perspective of the genetic basis for carbonyl stress resistance. *G3 (Bethesda)* **1**: 219–231.
- Jörnvall, H. (1970) Horse liver alcohol dehydrogenase. The primary structure of the protein chain of the ethanol-active isoenzyme. *Eur J Biochem* **16**: 25–40.
- Kasai, H., Iwamoto-Tanaka, N., and Fukada, S. (1998) DNA modifications by the mutagen glyoxal: Adduction to G and C, deamination of C and GC and GA cross-linking. *Carcinogenesis* **19**: 1459–1465.
- Kelly, J.M., and Wilkinson, S.R. (2013) Mechanisms of resistance to antiparasitic drugs in *Trypanosoma cruzi*. *Rev Española Salud Pública* **87**: 12–23.
- Kelly, J.M., Ward, H.M., Miles, M.A., and Kendall, G. (1992) A shuttle vector which facilitates the expression of transfected genes in *Trypanosoma cruzi* and *Leishmania*. *Nucleic Acids Res* **20**: 3963–3969.
- Kim, S.W., Li, Z., Moore, P.S., Monaghan, A.P., Chang, Y., Nichols, M., and John, B. (2010) A sensitive non-radioactive northern blot method to detect small RNAs. *Nucleic Acids Res* **38**: 1–7.
- Kwon, M., Lee, J., Lee, C., and Park, C. (2012) Genomic rearrangements leading to overexpression of aldo-keto reductase YafB of *Escherichia coli* confer resistance to glyoxal. *J Bacteriol* **194**: 1979–1988.
- Lange, J.N., Wood, K.D., Knight, J., Assimios, D.G., and Holmes, R.P. (2012) Glyoxal formation and its role in endogenous oxalate synthesis. *Adv Urol* **2012**: 5–9.
- Larsen, S.A., Kasseem, M., and Rattan, S.I. (2012) Glucose metabolite glyoxal induces senescence in telomerase-immortalized human mesenchymal stem cells. *Chem Cent J* **6**: 18.
- Lee, C., Kim, I., and Park, C. (2013) Glyoxal detoxification in *Escherichia coli* K-12 by NADPH dependent aldo-keto reductases. *J Microbiol* **51**: 527–530.
- Li, D., and Ellis, E.M. (2014) Aldo-keto reductase 7A5 (AKR7A5) attenuates oxidative stress and reactive aldehyde toxicity in V79-4 cells. *Toxicol in Vitro* **28**: 707–714.
- Li, D., Ferrari, M., and Ellis, E.M. (2012) Human aldo-keto reductase AKR7A2 protects against the cytotoxicity and mutagenicity of reactive aldehydes and lowers intracellular reactive oxygen species in hamster V79-4 cells. *Chem Biol Interact* **195**: 25–34.
- Macherey, A.-C., and Dansette, P.M. (2008) Biotransformations leading to toxic metabolites. Chemical aspect. In *The Practice of Medicinal Chemistry*. Wermuth, C.G. (ed.). Academic press, pp. 674–696.
- Marin-Neto, A.J., Rassi, A.J., Avezum, A., Mattos, A.C., and Rassi, A. (2009) The Benefit trial: testing the hypothesis that trypanocidal therapy is beneficial for patients with chronic Chagas heart disease. *Mem Inst Oswaldo Cruz* **104**: 319–324.
- Mejía-Jaramillo, A.M., Arboleda-Sánchez, S., Rodríguez, I.B., Cura, C., Salazar, A., Mazo, J., Del., *et al.* (2009) Geographical clustering of *Trypanosoma cruzi* I groups from Colombia revealed by low-stringency single specific primer-PCR of the intergenic regions of spliced-leader genes. *Parasitol Res* **104**: 399–410.

- Mejía-Jaramillo, A.M., Fernández, G.J., Palacio, L., and Triana-Chávez, O. (2011) Gene expression study using real-time PCR identifies an NTR gene as a major marker of resistance to benznidazole in *Trypanosoma cruzi*. *Parasit Vectors* **4**: 169.
- Mejía-Jaramillo, A.M., Fernandez, G.J., and Montilla, M. (2012) Sensibilidad al benznidazol de cepas de *Trypanosoma cruzi* sugiere la circulación de cepas naturalmente resistentes en Colombia. *Biomedica* **32**: 196–205.
- Mejía, A.M., Hall, B.S., Taylor, M.C., Gómez-Palacio, A., Wilkinson, S.R., Triana-Chávez, O., and Kelly, J.M. (2012) Benznidazole-resistance in *Trypanosoma cruzi* is a readily acquired trait that can arise independently in a single population. *J Infect Dis* **206**: 220–228.
- Murta, S.M., Gazzinelli, R.T., Brener, Z., and Romanha, A. J. (1998) Molecular characterization of susceptible and naturally resistant strains of *Trypanosoma cruzi* to benznidazole and nifurtimox. *Mol Biochem Parasitol* **93**: 203–214.
- Murta, S.M.F., Nogueira, F.B., Santos, P.F., Dos, Campos, F.M.F., Volpe, C., Liarte, D.B., et al. (2008) Differential gene expression in *Trypanosoma cruzi* populations susceptible and resistant to benznidazole. *Acta Trop* **107**: 59–65.
- Nogueira, F.B., Ruiz, J.C., Robello, C., Romanha, A.J., and Murta, S.M.F. (2009) Molecular characterization of cytosolic and mitochondrial trypanodioxidase in *Trypanosoma cruzi* populations susceptible and resistant to benznidazole. *Parasitol Res* **104**: 835–844.
- Parkinson, A., Ogilvie, B.W., Buckley, D.B., Kazmi, F., Czerwinski, M., and Parkinson, O. (2013) Biotransformation of Xenobiotics. In *Casarett & Doull's Toxicology, the Basic Science of Poisons*. Klaassen, C. (ed.). New York, NY: McGraw-Hill Education, pp. 133–224.
- Pascutti, M.F., Campodonico, G., García, F., Manarin, R., Bottasso, O., Revelli, S., and Serra, E. (2009) Novel cytostatic activity of the trypanocidal drug Benznidazole. *Int Immunopharmacol* **9**: 739–745.
- Pedrosa, R., Bem, A., De., and Locatelli, C. (2001) Time-dependent oxidative stress caused by benznidazole. *Redox Rep* **6**: 265–270.
- Penning, T.M. (2014a) The aldo-keto reductases (AKRs): overview. *Chem Biol Interact* **234**: 236–246.
- Penning, T.M. (2014b) Human aldo-keto reductases and the metabolic activation of polycyclic aromatic hydrocarbons. *Chem Res Toxicol* **27**: 1901–1917.
- Petrak, J., Ivanek, R., Toman, O., Cmejla, R., Cmejlova, J., Vyoral, D., et al. (2008) Déjà vu in proteomics. A hit parade of repeatedly identified differentially expressed proteins. *Proteomics* **8**: 1744–1749.
- Rodríguez, I.B., Botero, A., Mejía-Jaramillo, A.M., Marquez, E.J., Ortiz, S., Solari, A., and Triana-Chávez, O. (2009) Transmission dynamics of *Trypanosoma cruzi* determined by low-stringency single primer polymerase chain reaction and southern blot analyses in four indigenous communities of the Sierra Nevada de Santa Marta, Colombia. *Am J Trop Med Hyg* **81**: 396–403.
- Sandegren, L., Lindqvist, A., Kahlmeter, G., and Andersson, D.I. (2008) Nitrofurantoin resistance mechanism and fitness cost in *Escherichia coli*. *J Antimicrob Chemother* **62**: 495–503.
- Schmunis, G. A. (2007) Epidemiology of Chagas disease in non-endemic countries: the role of international migration. *Mem Inst Oswaldo Cruz* **102**: 75–85.
- Shangari, N., and O'Brien, P.J. (2004) The cytotoxic mechanism of glyoxal involves oxidative stress. *Biochem Pharmacol* **68**: 1433–1442.
- Shangari, N., Bruce, W.R., Poon, R., and O'Brien, P.J. (2003) Toxicity of glyoxals: role of oxidative stress, metabolic detoxification and thiamine deficiency. *Biochem Soc Trans* **31**: 1390–1393.
- Shangari, N., Chan, T.S., Popovic, M., and O'Brien, P.J. (2006) Glyoxal markedly compromises hepatocyte resistance to hydrogen peroxide. *Biochem Pharmacol* **71**: 1610–1618.
- Steindel, M., Neto, E.D., Pinto, C.J.C., Grisard, E.C., Menezes, C.L.P., Murta, S.M.F., et al. (1994) Randomly amplified polymorphic DNA (RAPD) and isoenzyme analysis of *Trypanosoma rangeli* strains. *J Eukaryot Microbiol* **41**: 261–267.
- Tenover, F.C. (2006) Mechanisms of antimicrobial resistance in bacteria. *Am J Med* **119**: S3–10–70.
- Tibayrenc, M., Ward, P., Moya, A., and Ayala, F.J. (1986) Natural populations of *Trypanosoma cruzi*, the agent of Chagas disease, have a complex multiclonal structure. *Proc Natl Acad Sci USA* **83**: 115–119.
- Ughes, D.I.H., and Ndersson, D.A.N.I.A. (1998) Virulence of antibiotic-resistant *Salmonella typhimurium*. *Proc Natl Acad Sci USA* **95**: 3949–3953.
- Upcroft, P., and Upcroft, J.A. (2001) Drug targets and mechanisms of resistance in the anaerobic protozoa. *Clin Microbiol Rev* **14**: 150–164.
- Verbon, E.H., Post, J.A., and Boonstra, J. (2012) The influence of reactive oxygen species on cell cycle progression in mammalian cells. *Gene* **511**: 1–6.
- Villarreal, D., Nirde, P., Hide, M., Barnabe, C., and Tibayrenc, M. (2005) Differential gene expression in benznidazole-resistant *Trypanosoma cruzi* parasites. *Antimicrob Agents Chemother* **49**: 2701–2709.
- WHO. (2015a) Chagas disease in Latin America: an epidemiological update based on 2010 estimates. *Wkly Epidemiol Rec* **90**: 33–44.
- WHO. (2015b) La enfermedad de Chagas (tripanosomiasis americana). <http://www.who.int/publications/es/>
- Wilkinson, S.R., Taylor, M.C., Horn, D., Kelly, J., and Cheeseman, I. (2008) A mechanism for cross-resistance to nifurtimox and benznidazole in trypanosomes. *Proc Natl Acad Sci USA* **105**: 5022–5027.
- Wyllie, S., Mandal, G., Singh, N., Sundar, S., Fairlamb, A.H., and Chatterjee, M. (2010) Elevated levels of trypanodioxidase in antimony unresponsive *Leishmania donovani* field isolates. *Mol Biochem Parasitol* **173**: 162–164.

Supporting information

Additional supporting information may be found in the online version of this article at the publisher's web-site.